Industrial Chemistry & Materials

ROYAL SOCIETY OF CHEMISTRY

PAPER

View Article Online
View Journal | View Issue

Check for updates

Cite this: *Ind. Chem. Mater.*, 2025, **3**, 231

Scalable manufacturing and reprocessing of vitrimerized flexible polyurethane foam (PUF) based on commercial soy polyols†

Wangcheng Liu,[a] Yaqiong Zhang,[a] Peter Chen,[a] Lin Shao,[a] Yiding Cao,[a] Baoming Zhao,[a] Ellen C. Lee,[b] Xiaojiang Wang[b] and Jinwen Zhang *[a]

As the polyurethane foam (PUF) market, especially in the automotive sector, continues to grow, the environmental impacts of its petrochemical demands and end-of-life waste have motivated the industry to look for more sustainable solutions. This study explores the preparation of recyclable PUFs using commercially available soy polyols (Cargill's BiOH), aiming to enable improved thermal reprocessability of flexible PUFs *via* vitrimer chemistry. A series of "soy-PUFs" was produced by partially substituting petrochemical polyether polyols with 25% or 50% soy polyols in a standard reference formulation. Incorporation of soy polyols resulted in an increase in the stiffness of the resulting foams. Employing a modest amount (~0.5 wt%) of dibutyltin dilaurate (DBTDL) in the formulations facilitated dynamic covalent bond exchanges in the cross-linked network during a mild "foam-to-sheet" reprocessing process (160 °C), converting malleable PUFs into densified sheet materials (PUS) with proper compactness and mechanical performance (*e.g.*, tensile modulus = ~50 MPa). Soy-PUFs demonstrated a modestly enhanced stress relaxation behavior, suggesting adequate reprocessing ability. DMA results demonstrated the phenomenon of forming an "intermediate" region between the hard and soft domains of PUSs after reprocessing.

Received 14th September 2024,
Accepted 27th December 2024

DOI: 10.1039/d4im00117f

rsc.li/icm

Keywords: Polyurethane foam; Soybean oil; Polyols; Vitrimer chemistry; Reprocessing; Recycling.

Open Access Article. Published on 22 1403. Downloaded on 10/03/1405 06:34:15 ..
This article is licensed under a Creative Commons Attribution-NonCommercial 3.0 Unported Licence.

1 Introduction

Polyurethane foams (PUFs) are a very important class of polyurethane (PU) products and have found a wide range of applications in automotives, footwear, building, furniture, sealing, adhesion, and packaging.[1–3] The utility and versatility of PUFs are often based on their unique characteristics, *i.e.*, customizable porosity and density, adjustable cushioning resiliency, and thermal and acoustic insulation. Flexible PUFs play an important role in the automotive industry due to their contributions to light weight, passenger comfort, airflow filtration, damping, and sound insulation.[2,4–6] In addition to established automotive applications, PUFs have good potential in different fields such as building insulation and construction materials (*e.g.*, spray foam), packaging products for cushioning, and furniture.[7] The global market size of PUFs reached about $40 billion in 2020.[8,9]

The growing demand for PUFs brings environmental concerns related to their petrochemical origins and the challenges of waste management. In order to reduce the carbon footprint, efforts have been made to use biobased alternatives in PUF formulations, such as plant-based natural oil polyols.[8,10–22] Soybean oil-based polyols (*i.e.*, soy polyol) have been commercially successful in the marketplace, offering a range of properties for PUFs suitable for various applications by tailoring the molecular architecture of soy polyols, like OH values, molecular weights (M_W), and OH functionalities.[15,23–29] One of the most established techniques for synthesizing soy polyols is the epoxidation of double bonds of soybean oils, followed by the opening of the oxirane rings by nucleophilic monoalcohols (*e.g.*, methanol). For instance, the Cargill company developed a series of soy polyols (*e.g.*, BiOH® series) with different OH values from 28 to 224 mg KOH g^{-1} and hydroxyl functionalities of 0.48–4.9.[30] Nevertheless, the actual loads of soy polyols in industrial PUF products remain modest, typically ranging from 5 to 15 wt%, primarily due to the consideration of cost and potential compromises in material performance and cellular structure.[6,8,31–36]

[a] *Composites Material and Engineering Center, Washington State University, Pullman, Washington, 99164, USA. E-mail: jwzhang@wsu.edu*
[b] *Research and Advanced Engineering, Ford Motor Company, Dearborn, Michigan, 48124, USA*

† Electronic supplementary information (ESI) available. See DOI: https://doi.org/10.1039/d4im00117f

© 2025 The Author(s). Co-published by the Institute of Process Engineering, Chinese Academy of Sciences and the Royal Society of Chemistry

Open Access Article. Published on 22 1403. Downloaded on 10/03/1405 06:34:15 ..
This article is licensed under a Creative Commons Attribution-NonCommercial 3.0 Unported Licence.

In the USA, only 5.5% of PU materials were effectively recycled,[9] while the true recycling rate for PUFs was likely to be even lower due to their cross-linked nature. Current recycling technologies of PUFs generally fall into two categories: mechanical or chemical routes.[1,2,37–42] Mechanical recycling, such as re-grinding of PUFs as polymeric composite fillers and press re-bonding of PUFs with binders (*e.g.*, more isocyanate resins), is often considered "downcycling" since only low-value products (*e.g.*, carpet underlays) will be generated. Chemical recycling, which depolymerizes PUFs into oligomers and monomers for another production cycle,[43] faces hurdles in energy consumption, usage of hazardous solvents (*e.g.*, alkanolamines) and catalysts, and low recycling yields since the hard segments of PUFs are usually separated from the recyclates (mostly polyols) and eventually disposed of as chemical waste.[2,38,44–46] In addition, in recent years, some studies have also suggested that biological degradation is another promising approach for the comprehensive waste management of PUF.[47,48]

New technologies are needed to promote the recycling of end-of-life PUFs. Recent studies have explored the utilization of covalent adaptable networks (CANs) as a means to improve the processability of thermosets.[49–58] The "vitrimerization" of cross-linked PU materials offers a more eco-friendly and cost-effective solution for recycling PUFs, as well as has the potential to achieve a 100% recycling yield, filling the gap for chemical recycling. Nevertheless, compared to other types of cross-linked PU materials, little effort has been made to date in PUFs.[42,59] When heated beyond the service temperatures (*e.g.*, >180 °C), traditional PUFs can be reprocessed to a certain degree due to (1) the long-chain soft segments (polyols), which may provide somewhat thermoplastic behavior;[37,38] (2) the carbamate bonds of PUFs are inherently subject to dynamically exchangeable reaction in the presence of catalysts.[56,58,60–64] Because the concentration of catalyst is usually low in foam products (*e.g.*, <0.75 wt%), the topological rearrangement of PUFs is usually slow and cannot complete within a normal reprocessing cycle time (*e.g.*, <1 hour).[59,65,66]

In this work, vitrimerized PUFs were introduced by utilizing commercially available soy polyols (Cargill's BiOH®) within standard industrial frameworks, and their properties and thermal reprocessability were thoroughly investigated. Soy polyols accounted for 14–29 wt% of the total mass of the foam, which was well above soy polyol content in current commercial products (usually 5–20%), according to Cargill's own sources.[30] Dibutyltin dilaurate (DBTDL) was used as the catalyst for both curing in foam preparation and reprocessing of the foam waste, and its content was roughly 0.5 wt% in all formulations. The stoichiometry was slightly imbalanced with a –OH/–NCO molar ratio of 0.98, which favored the transcarbamoylation at elevated temperature and hence facilitated the "foam-to-sheet" (160 °C for 30 minutes at 15 MPa) reprocessing. The resulting sheets (PUSs) displayed mechanical properties comparable to those of other commercial PU products. Technical challenges and knowledge gaps were elaborated to give a comprehensive insight into the balance between operational feasibility and sustainability in the entire life cycle of PUFs, advocating for the broader adoption of soy polyol-based PUFs (*i.e.*, so-PUFs) in the commodity marketplace and recycling of end-of-life products.

2 Result and discussion

2.1 Preparation and properties of PUFs

We first prepared 7 formulations of PUFs varying the selection and content of polyols. One of the PUF samples was regarded as the control formulation and named F-Control ("F" represents foam), which was prepared from petrochemical polyether polyol Voranol® 4701 alone; the other 6 PUF samples in which soy polyol replaced either 25 wt% or 50 wt% Voranol 4701 were noted as "soy-PUFs", where the notation of "aa%bb" indicates the content ("aa") and selection of the soy polyol ("bb"). For these soy-PUFs, soy polyol-1 (BiOH® 5000) with a lower OH functionality of 1.7 and soy polyol-2 (BiOH® 5300) with a higher OH functionality of 3.0 were either applied individually (F-25%50, F-50%50, F-25%53, and F-50%53) or together in a blend of a 1 : 1 weight ratio (F-25%Bo and F-50%Bo, where "Bo" means both). To differentiate between the PU sample before and after reprocessing, foams (PUFs) were named "F-*x*" (*e.g.*, F-Control and F-50%Bo), while sheets (PUSs) obtained from the "foam-to-sheet" process were named "S-*x*" (*e.g.*, S-Control and S-50%Bo). As illustrated in Fig. 1a, commercial soy polyols, BiOH 5000 and/or BiOH 5300, were blended with petrochemical polyether polyol (Voranol 4701) and then reacted with MDI to synthesize soy-PUFs. PUF samples with a weight of 75 grams for characterization and analysis and a weight of 300 grams for demonstration of scalability were both manufactured.

Fig. 1b shows the FTIR curves of the PUF samples. Although –OH was slightly in excess with respect to –NCO at a molar ratio of 1 : 0.98, a small peak at 2270 cm^{-1} can be identified as unreacted remaining –NCO groups from MDI in the PUFs (Fig. S1†). A similar observation of a trace amount of residual –NCO in PUFs is also reported in the literature.[18,22,36,67–73] This could be due to the common microphase separation between the hard domain (water-MDI-DEA) and the soft domain (polyether polyol) during the gelation, leaving small amounts of unreacted –OH and –NCO groups. The spectrum in the range of 1620–1800 cm^{-1} attributed to the stretch vibrations of carbonyl (–C═O) is of interest (Fig. 1c). The F-Control, a polyether-based PUF, shows multiple peaks, such as free and hydrogen-bonded carbamates (urethane bonds) at ~1700–1735 cm^{-1} and free and hydrogen-bonded (monodentate and bidentate) carbamides (urea bonds) at 1640–1715 cm^{-1}.[21,33,52,74–76] In comparison, soy-PUF shows an intensified shoulder at 1740 cm^{-1} attributed to the carbonyl stretching vibration of ester bonds in the soy polyols, as confirmed by the IR spectra of polyols (Fig. S1†). Correspondingly, soy-PUFs exhibit lower peak intensities of ether stretching vibrations at 1090 cm^{-1},[36,70,77,78] though soy polyol also contains a small amount of ether bonds.

Fig. 2 and S2† show the microcellular structure of PUFs, examined using SEM and optical microscopy. Based on a measurement of approximately 400 pores, it was noted that the cell sizes (Φ) of soy-PUFs were smaller than that of the F-Control. For instance, the average diameter of the F-Control

© 2025 The Author(s). Co-published by the Institute of Process Engineering, Chinese Academy of Sciences and the Royal Society of Chemistry

Open Access Article. Published on 22 1403. Downloaded on 10/03/1405 06:34:15 ..
This article is licensed under a Creative Commons Attribution-NonCommercial 3.0 Unported Licence.

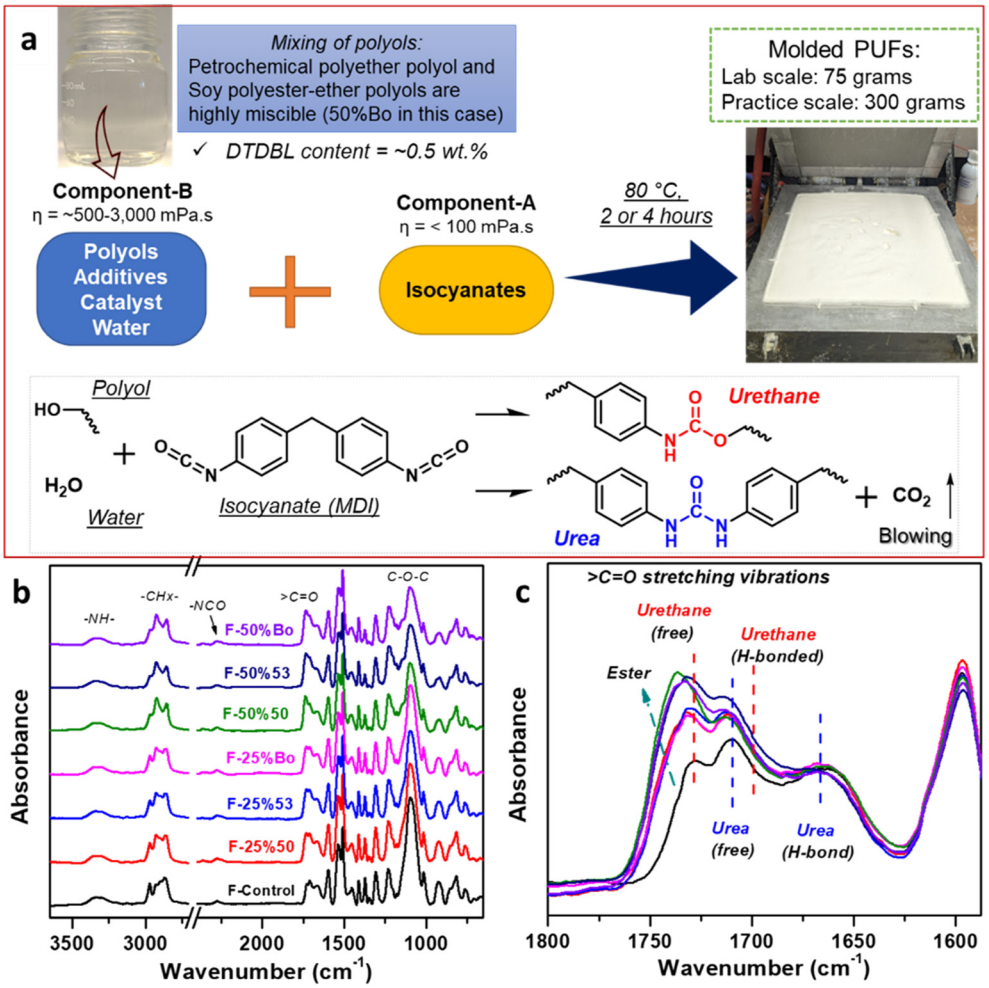

Fig. 1 (a) Synthesize and fabrication of soy-PUFs; (b) FTIR spectra of PUF samples, in which (c) the carbonyl stretching vibrations at 1600–1800 cm^{-1} are noted.

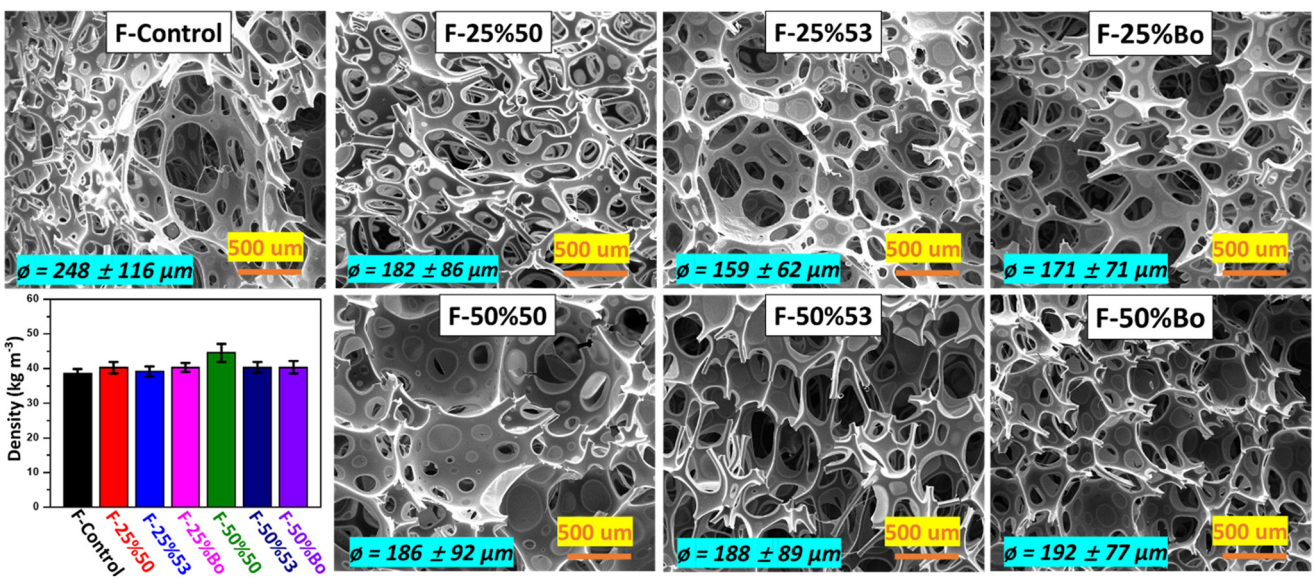

Fig. 2 SEM images (magnitude: 100×) and the apparent densities of PUF samples.

© 2025 The Author(s). Co-published by the Institute of Process Engineering, Chinese Academy of Sciences and the Royal Society of Chemistry

Open Access Article. Published on 22 1403. Downloaded on 10/03/1405 06:34:15 ..
This article is licensed under a Creative Commons Attribution-NonCommercial 3.0 Unported Licence.

was 248 μm, while this value for F-25%53 was reduced by 36% to 159 μm. Soy-PUFs have smaller cell sizes because the higher viscosities of soy polyols (Fig. S1†) could limit cell growth and reduce "cell drainage" by gravity (uncured liquid mixtures move downward by gravity) during the foaming process.[4,21,36,69,79,80] However, this trend was almost negligible when 50% soy polyols were introduced. A high level of cell openness prevents the foam from shrinking during curing, influencing the cushioning quality and breathability of the final products.[8,81] While the F-50%50 same has a higher fraction of closed cells (Fig. S2†), the other 5 soy-PUF samples have similar open cell fraction ratios as the F-Control. Although the addition of soy polyols affected the microcellular structure of PUFs, the flexible soy-PUFs exhibited similar apparent densities (Fig. 2) as the F-Control (38–41 kg m^{-3}), except for F-50%50 with a higher density of 44.5 kg m^{-3} that could be attributed to its lower cell openness.

It can be argued that commercially available soy polyols have been optimized for forming internal microcellular structures, fluid flowability prior to gelation, and stability to prevent foam shrinkage. In comparison, some lab-made bio-based polyols may face challenges in stabilizing cell opening and preventing foam shrinkage.[8,22,79,82,83] The types and concentrations of catalysts, surfactants, and cell openers were kept unchanged in all the 7 formulations to keep consistency. The compositions of the PUF formulations are detailed in Tables S1 and S2.† It is a common practice in industry to adjust these additives to optimize cell morphology, but no such adjustments were made in our experiment to ensure the consistency of the formulations.

Incorporation of plant oil-based polyols in preparation of flexible PUFs may change the inherent softness. It is recognized that soy polyols with low OH value, low OH functionality, and high molecular weight are crucial for achieving flexible PUFs. Empirically, OH functionality of 2 for soy polyols is considered a threshold level in flexible PUFs. A higher OH functionality can result in a more rigid network structure and thereby impart excessive mechanical stiffness,[19,20] whereas a lower OH functionality is incapable of completing the cross-linked networks. In general, the molecular structure of soy polyol significantly influences the mechanical properties of resulting flexible PUFs. Fig. 3a and b are stress–strain curves from the tensile and compression deflection tests of PUFs, and the results are summarized in Tables 1 and S3.† The F-50%53 exhibited the highest tensile modulus and strength (794.7 and 146.1 kPa), which are about 4 and 1.8 times that of the F-Control (186 and 83.6 kPa). Correspondingly, the elongation

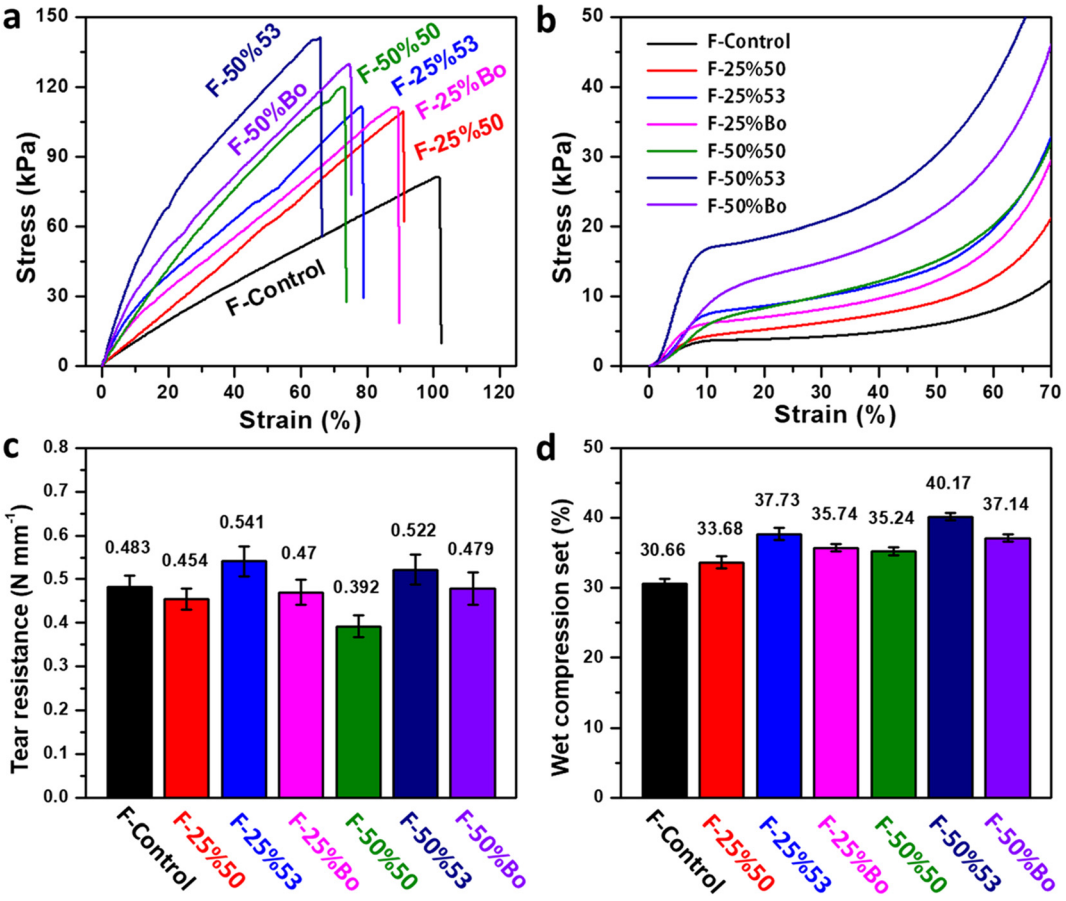

Fig. 3 (a) Tensile stress–strain curves; (b) compression stress–strain curves; (c) tear resistance; and (d) wet compression set of PUF samples.

© 2025 The Author(s). Co-published by the Institute of Process Engineering, Chinese Academy of Sciences and the Royal Society of Chemistry

Open Access Article. Published on 22 1403. Downloaded on 10/03/1405 06:34:15 ..
This article is licensed under a Creative Commons Attribution-NonCommercial 3.0 Unported Licence.

Table 1 Tensile properties and tear resistance of PUFs

Code	Tensile properties			Tear resistance (N mm^{-1})
	Young's modulus (kPa)	Stress at break (kPa)	Ultimate elongation (%)	
F-Control	186.0 ± 23.3	83.6 ± 6.9	95.7 ± 12.2	0.483 ± 0.026
F-25%50	234.7 ± 35.8	110.2 ± 4.4	90.4 ± 7.3	0.454 ± 0.024
F-25%53	445.4 ± 32.9	120.3 ± 8.3	76.4 ± 12.5	0.541 ± 0.034
F-25%Bo	355.3 ± 45.5	122.1 ± 7.9	90.2 ± 11.7	0.470 ± 0.029
F-50%50	357.9 ± 30.3	117.5 ± 8.4	74.6 ± 8.3	0.392 ± 0.025
F-50%53	794.7 ± 71.9	146.1 ± 11.8	65.3 ± 5.7	0.522 ± 0.034
F-50%Bo	510.0 ± 46.0	129.8 ± 6.1	79.1 ± 5.8	0.479 ± 0.037

of soy-PUFs decreased. Likewise, soy-PUFs show much higher compression modulus and strength, where the effect of BiOH 5300 (F-25%53 and F-50%53) is more noticeable over BiOH 5000 (F-25%50 and F-50%50). For instance, the compression modulus of F-50%Bo is 510 kPa (Table S3†), a ~175% increase from the F-Control of 186 kPa.

Tear resistance represents the ability of PUFs to resist the crack propagation caused by deformation, indicating long-term reliability throughout the service life. Fig. 3c shows the tear resistance of PUFs. The F-25%50 sample showed a similar tear resistance (0.454 N mm^{-1}) as the F-Control (0.483 N mm^{-1}), while F-50%50 even had a lower tear resistance (0.392 N mm^{-1}). On the contrary, both foam samples containing BiOH 5300 exhibit enhanced tearing strength of PUFs (0.541 and 0.522 N mm^{-1}). One possible reason is that BiOH 5300 has higher OH functionality than BiOH 5000 (3.0 *vs.* 1.7), constructing a more robust network structure to resist mechanical damage and improving the interfacial cohesiveness between the soft domain (long-chain polyether polyols) and the hard domain (aromatic isocyanates).[84] When these two soy polyols were blended, both F-25%Bo and F-50%Bo achieved a moderate tear resistance of 0.470 and 0.479 N mm^{-1}, respectively.

Another parameter for assessing the aging durability of flexible PUFs is the wet compression set, where the PUFs undergo compressive deformation in a humid environment, and their ability to recover their original structure is measured. As shown in Fig. 3d, the F-Control has the lowest compression set value of 30.6. When the Voranol was replaced by 50 wt% BiOH, the wet compression set of soy-PUFs increased, indicating that more permanent deformation occurred. Indeed, soy polyols, especially BiOH 5300, increased the rigidity of the PU networks, enhancing plasticity and reducing mechanical resiliency after aging. These values suggest that these soy-PUFs are suitable for underbody thermal and acoustic insulation (typically set value around 50%) in automotive applications, but exceed the compression set of seat cushions (typically set value < 30%).[4]

2.2 Dynamic mechanical properties and stress relaxation of PUFs

Due to the molecular architecture, plant oil-based polyols may not constitute the soft domain of flexible PUFs with long-chain polyether polyols, even if they are miscible. For example, Macosko *et al.*[33] reported a flexible soy-PUF using soy polyol of similar structure but having a higher OH functionality than BiOH 5300 (3.8 *vs.* 3). The soy segments eventually formed a "secondary" soft domain in the flexible PUFs, as reflected in a very broad damping (tan δ) peak at ~75 °C. At the same time, the glass transition associated with the long-chain polyether polyol remained unchanged at −45 °C. However, data on flexible PUFs using soy polyols with lower OH functionality (*e.g.*, ~2) is scarce, indicating the need for further investigation.

Fig. 4 shows the changes of storage modulus, (E', 4a) and damping factor (tan δ, 4b) with temperature measured from DMA test for PUF samples. The F-Control exhibited a classic soft–hard segmented phenomenon of PU materials: one transition for the soft domain (polyether polyols) at −35 °C and another for the hard domain (water-MDI-DEA) above 200 °C. The temperature of the DMA experiment was kept below 200 °C to avoid decomposition of the PUF sample on the instrument.[35] On the other hand, the changes of slops in E' and tan δ indicate that the glass transition of hard domains (T_g2) in all formulations began at about 150–160 °C, paving the way for topological rearrangement (*i.e.*, Tv). Likewise, Kurańska *et al.* reported that the tan δ peaks of palm oil-based rigid PUFs were higher than 200 °C.[85] The addition of soy polyols, especially BiOH 5300 (OH value = 117 mg KOH g^{-1}), resulted in broadening the first glassy-rubbery transition (T_g1) of PUFs. For instance, F-50%53 exhibited a damping factor that gradually increased from −60 °C across the entire transition range, while the peak intensity at −35 °C was dramatically depressed. The T_g1 peak of sample F-25%53 shifted significantly from that of the F-Control (−35 °C) to −18 °C, behaving similarly to the flexible PUFs made from palm oil polyol with a high OH value of 134 mg KOH g^{-1}.[86] In sharp contrast, the E' and tan δ curves of F-25%50 are similar to those of the F-Control, aligning with flexible PUFs using only 5–20% modified castor oil polyol (reduced OH content than virgin castor oil) with a low OH value of 79.4 mg KOH g^{-1} and OH functionality of 2.[87] To preserve the inherent softness and resiliency of flexible PUFs, the plant oil-based polyols with high Mw (*e.g.*, 3000–6000 g mol^{-1}), low OH value (*e.g.*, <100 mg KOH g^{-1}), and relatively low OH functionality (but still higher than 2) are preferred.[20] For instance, Yang *et al.* observed that the T_g of PU soled based

© 2025 The Author(s). Co-published by the Institute of Process Engineering, Chinese Academy of Sciences and the Royal Society of Chemistry

Open Access Article. Published on 22 1403. Downloaded on 10/03/1405 06:34:15 ..
This article is licensed under a Creative Commons Attribution-NonCommercial 3.0 Unported Licence.

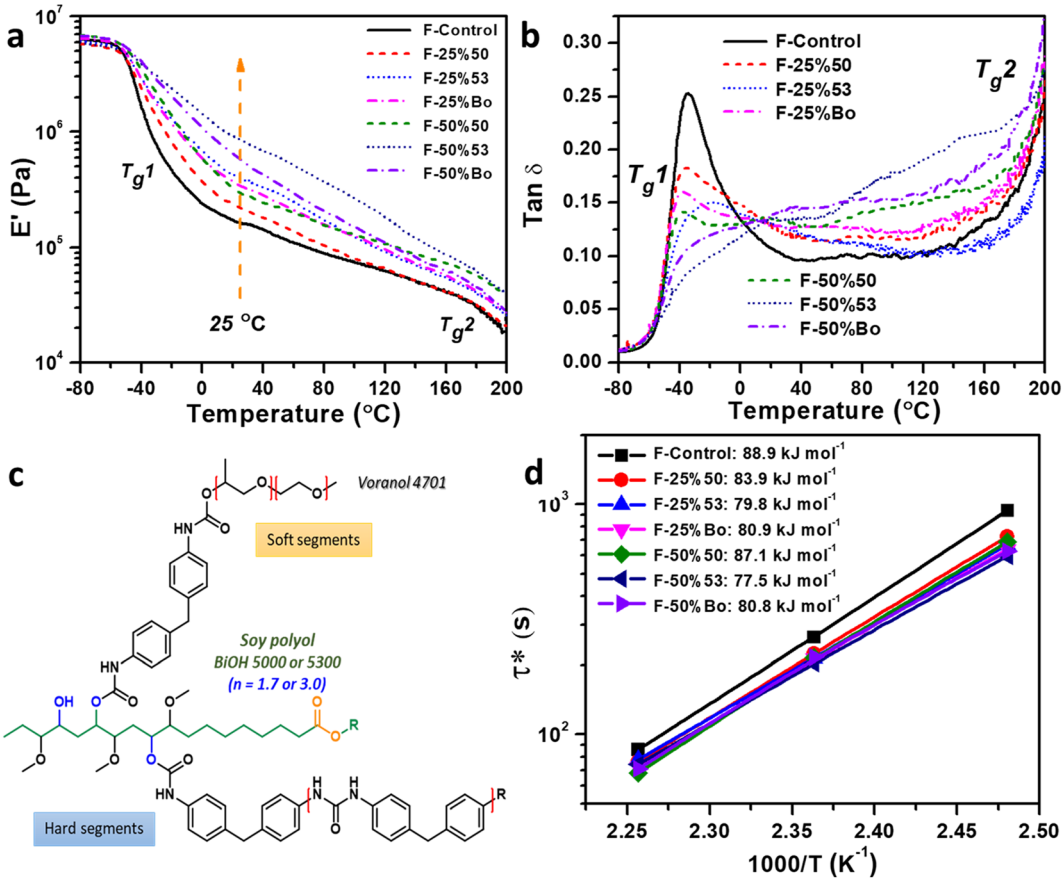

Fig. 4 (a and b) DMA curves of PUF samples as a function of temperatures, including (a) E' and (b) tan δ; (c) schematic diagram of molecular architecture in soy-PUFs, where the soy segments were represented by linolenic esters; (d) fitting of relaxation time (τ^*) to Arrhenius equation and the calculated apparent activation energy (E_a) for PUFs.

on a soy polyol with an OH functionality of 2.6 was 21 °C.[88] Apparently, BiOH 5000 (OH value = 56 mg KOH g^{-1}) meets this flexibility criterion, but its lower OH functionality of 1.7 also leads to a reduced cross-link degree of PUFs, as indicated by its low gel contents (Table S4†).

The glass transition associated with the rigid segment domain is also influenced by incorporating soy polyols. The most obvious example is still F-50%53, as its tan δ curve shows an upward trend starting at ~60 °C. This is probably due to the wide molecular weight distribution of soy polyols, a common challenge in converting plant-oils into polyols through epoxidation, which can lead to the formation of oligomers.[19,20,89–92] In our case, BiOH 5000 and BiOH 5300 have a large polydispersity index (PDI) of over 3.5 (Fig. S1†). It can be assumed that the fractions of lower or higher molecular weight soy polyols could affiliate with either hard or soft segments, respectively. As a result, the soy segments created "intermediate regions" between soft domain and hard domain during the microphase separation of soy-PUFs (Fig. 4c).

Dynamic covalent bond interchanges determine the stress relaxation and, hence, the reprocessability of PUFs. Fig. S3† shows stress relaxation of PUF at 130, 150, and 170 °C. The F-Control demonstrated stress relaxation times τ^* (at G/G_0 = 1/e) of 952, 265, and 86 s at 130, 150, and 170 °C, respectively, with an activation energy f of 88.9 kJ mol^{-1} (Fig. 4d). Because the PUF in this study contained approximately 0.45 wt% DBTDL in addition to tertiary amine catalysts the activation energy of the F-Control sample was lower than that (~120 kJ mol^{-1}) of typical PUFs reported in the literature,[59,66,93] but still higher than that of some PUFs loaded with extra catalysts aimed for the reprocessing purposes (~40–60 kJ mol^{-1}).[94,95] On the other hand, despite their intrinsic network rigidity, soy-PUFs at elevated temperatures exhibited faster relaxation, as seen in approximately 10–20% reductions in relaxation time, like 68 s at 170 °C (F-50%53). This could be attributed to the potential transesterification within the PU networks. Among these 6 soy-PUF samples, the activation energies of F-25%53 and F-50%53 (below 80 kJ mol^{-1}) are lower than those of F-25%50 and F-50%50 (beyond 80 kJ mol^{-1}). The PUFs made from BiOH 5300 had relatively higher gel contents of ~97% (Table S4†) due to the high OH functionality, yet F-25%53 and F-50%53 still exhibited faster relaxation. This was attributed to the increased contents of –OH groups and carbamate bonds (Table S2†) in the foam products, accelerating transcarbamoylation and urethane exchange at elevated temperatures.

© 2025 The Author(s). Co-published by the Institute of Process Engineering, Chinese Academy of Sciences and the Royal Society of Chemistry

Open Access Article. Published on 22 1403. Downloaded on 10/03/1405 06:34:15 ..
This article is licensed under a Creative Commons Attribution-NonCommercial 3.0 Unported Licence.

2.3 Foam-to-sheet thermal reprocessing

Reprocessing of PUFs by leveraging dynamic covalent chemistry has received a lot of attention in the literature. The reprocessing can be realized by traditional compression molding[66,93,94,96] or extrusion[46,59,95,97] techniques to achieve the "foam-to-sheet" or "foam-to-film" conversion, often at processing temperatures up to 200 °C. While extrusion reprocessing is advantageous in a continuous process, its realization requires an excessive amount of catalyst (*e.g.*, >2 wt%) before reprocessing to achieve rapid relaxation in typical polyether-based PUFs. There will be some technical challenges to prepare PUF with high catalyst concentration or to load more catalysts to the PUF afterward. Reprocessing through compression molding, like in this study, requires much less catalyst (Fig. 5a), like 0.5 wt% described in Table S1.†

End-of-life PUFs typically undergo the shredding process to obtain big fragments or pulverization to give fine ground powders for reuse in polymeric composites. The pulverizing of the scrapped PUF waste can produce particles with a more uniform size and shape that is more convenient for reprocessing operations, but it consumes more energy. In this regard, we first focused on the low-energy shredding process, and the results of PUSs after foam-to-sheet reprocessing of shredded PUF fragments were demonstrated and discussed. Here, shredded PUF fragments were molded at 160 °C for 40 min (30 min hot-press and 10 min cold-press) to be densified into sheet materials (*i.e.*, PUSs, named S-*x*).

The morphology of densified PUSs was examined by optical microscopy (surface of samples) and SEM (internal structure of samples), as illustrated in Fig. 5b. All 7 PUS samples displayed very similar densities of approximately 1.1 g m^{-3}. This could be attributed to the successful topology rearrangement mainly facilitated by DBTDL-catalyzed transcarbamoylation. For soy-PUFs, the transesterification of ester bonds could further contribute to the topology rearrangement during reprocessing. Thus, from a macroscopic perspective, the microcellular structure was eradicated, endowing the PUS samples with adequate structural integrity and compactness. Nevertheless, some samples (especially S-50%50) showed internal cracks might be related to the remnants of the original microcellular structure (marked in the figure), though these cracks had been healed by the decent thermoplastic-liked malleability of vitrimers, resulting in a welding-like morphology. Notably, S-25%50 and S-50%50 exhibit poorer phasic homogeneity and more cracks (see optical microscopy images) than the other 5

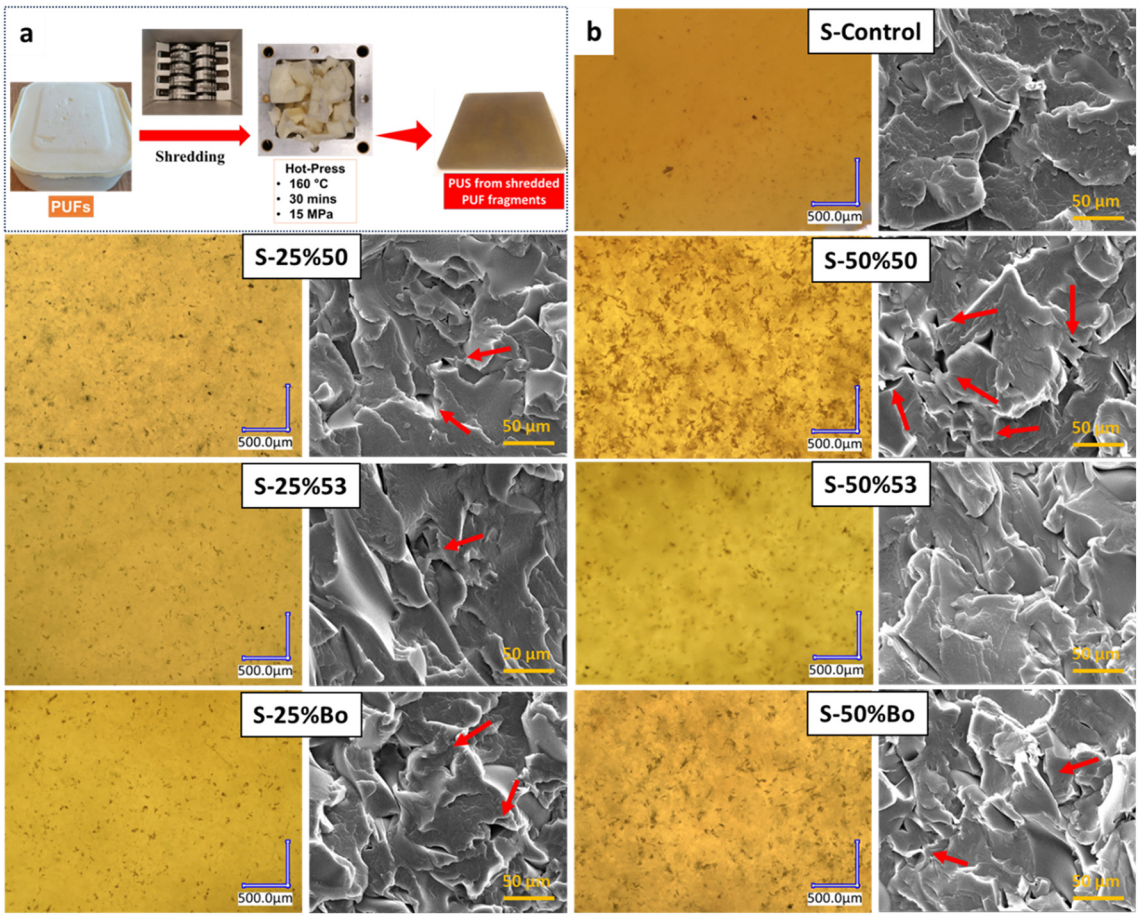

Fig. 5 (a) Foam-to-sheet conversion of shredded PUF fragments into PUSs *via* compression molding; (b) optical images (magnification: 100×) of the surfaces of as-molded PUSs and SEM images of cryo-fractured samples (magnification: 1000×) of PUSs. The red arrows mark the voids.

© 2025 The Author(s). Co-published by the Institute of Process Engineering, Chinese Academy of Sciences and the Royal Society of Chemistry

Open Access Article. Published on 22 1403. Downloaded on 10/03/1405 06:34:15 ..
This article is licensed under a Creative Commons Attribution-NonCommercial 3.0 Unported Licence.

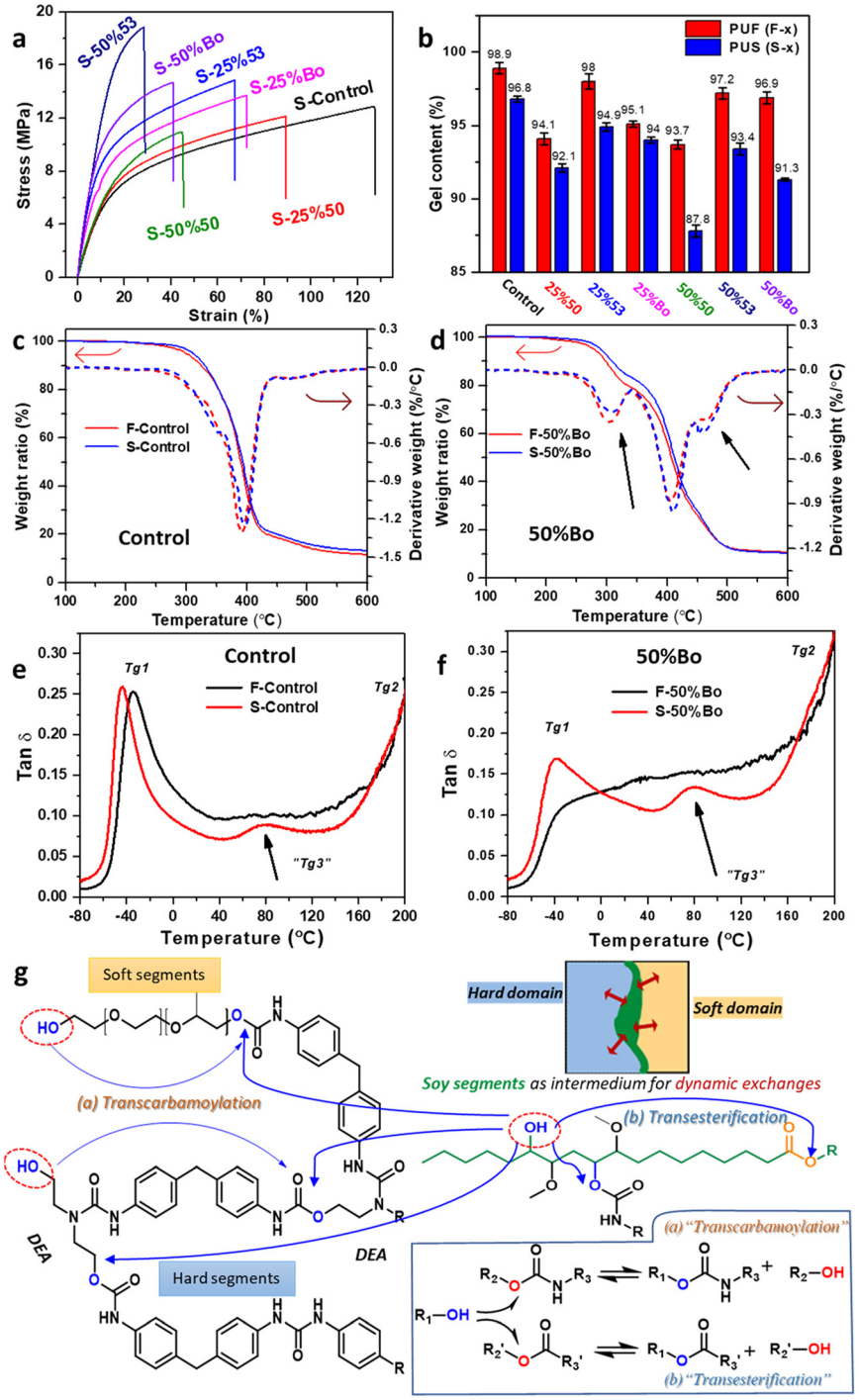

Fig. 6 (a) Stress–strain curves of PUSs; (b) gel contents of PUFs and PUSs; (c) TGA and DTG curves of F-Control *vs.* S-Control; (d) TGA and DTG curves of F-50%Bo *vs.* S-50%Bo, the arrows marked the difference between Control and 50%Bo (both PUFs and PUSs); (e) tan δ of F-Control *vs.* S-Control, the arrows marked the emerge of "T_g3"; (f) tan δ of F-50%Bo *vs.* S-50%Bo, the arrows marked the emerge of "T_g3"; (g) schematic diagram of the dynamic bond exchanges in the PU networks, including (g/a) transcarbamoylation and (g/b) transesterification reactions.

PUS samples, leading to inferior mechanical performance, as further discussed below.

PUS samples show tensile behaviors ranging from flexible to semi-rigid, depending on specific composition (Fig. 6a and Table 2). For instance, S-Control demonstrated a modulus of 31.3 MPa, a strength of 12.8 MPa, and the highest elongation of 134%, analogous to hard rubber materials. On the contrary, S-50%53 exhibited the highest modulus and strength of 120.9 and 18.2 MPa, respectively, while its elongation was only 28%, showing a semi-rigid feature. In addition, the Shore D hardness for S-50%53 increases by approximately 50% to 48.6, compared to 32.3 for the S-Control. However, the mechanical properties of

© 2025 The Author(s). Co-published by the Institute of Process Engineering, Chinese Academy of Sciences and the Royal Society of Chemistry

Open Access Article. Published on 22 1403. Downloaded on 10/03/1405 06:34:15 ..
This article is licensed under a Creative Commons Attribution-NonCommercial 3.0 Unported Licence.

Table 2 Density, tensile properties, and Shore D hardness of PUSs

Code	Density (g cm^{-3})	Tensile properties			Shore D hardness
		Modulus (MPa)	Strength (MPa)	Elongation at break (%)	
S-Control	1.13 ± 0.02	31.3 ± 2.3	12.8 ± 1.6	134 ± 16	32.3 ± 0.4
S-25%50	1.09 ± 0.02	31.9 ± 2.7	11.6 ± 0.8	87 ± 10	33.5 ± 0.8
S-25%53	1.08 ± 0.02	71.4 ± 5.0	14.8 ± 1.3	68 ± 11	38.8 ± 0.6
S-25%Bo	1.11 ± 0.03	50.9 ± 1.9	13.3 ± 1.4	71 ± 9	34.3 ± 0.6
S-50%50	1.09 ± 0.02	38.9 ± 3.3	10.4 ± 0.9	43 ± 3	34.1 ± 1.0
S-50%53	1.10 ± 0.03	120.9 ± 8.9	18.2 ± 1.1	28 ± 4	48.6 ± 1.0
S-50%Bo	1.09 ± 0.02	88.7 ± 5.8	14.9 ± 0.9	36 ± 4	41.0 ± 0.8

S-25%50 and S-50%50 were somewhat unsatisfactory, likely due to the presence of internal cracks and voids observed in SEM images (Fig. 5b). Because the average OH functionality of BiOH 5000 is only 1.7, its inclusion in the preparation of foam would result in the formation of defects, *i.e.*, some dangling segments, in the network structure. The dynamic transesterifications during reprocessing of the PUF are likely to cleave some of those dangling segments, as illustrated in Fig. S4,† resulting in the deterioration of mechanical properties. For instance, S-50%50 has the lowest gel contents of 87.8% (in toluene), while this value is 96.8% and 93.4% for S-Control and S-50%53, respectively (Fig. 6b and Table S4†). The cleavage of dangling segments reduces the effectiveness of dynamic covalent bond exchange-induced healing at interfaces. This phenomenon is not frequently addressed in other studies of biobased vitrimers using plant oil as raw compounds.

The results from the TGA experiment indicate that soy-PUFs and their derived PUSs (Fig. 6d, using F-50%Bo and S-50%Bo as examples) were more vulnerable to thermal degradation than the Control formulations (Fig. 6c, F-Control and S-Control), indicating the reduced thermal stability due to the presence of soy segments in the cross-linked networks. This observation is in good agreement with that from other studies on some biobased PUFs.[8,18,22,68] For instance, the temperature of 5% weight loss (T_{d5}) for S-50%Bo was 281.5 °C, which was about 20 °C lower than that for the S-Control (301.1 °C). The decomposition of soybean oil segments was more pronounced from the DTG curves, as it peaked at ~285–310 °C (marked in the figure). In fact, we observed that an oily substance was released when the reprocessing temperature was 180 °C or higher (Fig. S4†), possibly fatty compounds and glycerol. This result also suggests that the faster stress relaxation behavior of soy-PUFs (especially for F-50%50) at higher temperatures (*e.g.*, >170 °C) may not provide precise information regarding reprocessability because of the degradation issue. Furthermore, S-50%Bo showed another decomposition at ~475 °C (marked in the figure), which might be related to the soy segments linked with the hard domain having better thermal stability than those in the soft domain (~300 °C). From DTG curves, we concluded that PUSs after reprocessing had similar thermal properties to the original PUFs.

Fig. 6e and f show the comparison of damping behaviors between PUFs and PUSs. Interestingly, a "3rd" glass transition (T_g3, ~80 °C) is also noted in the S-Control (Fig. 6e), which could be attributed to the formation of an "intermediate" domain *via* dynamic covalent bond exchanges as illustrated schematically in Fig. 6g. The main mechanism for vitrimerization of PUFs was DBTDL-catalyzed transcarbamoylation of carbamate bonds in the presence of free –OH groups in the PU networks, associated with urethane exchanges.[56–59,91] For soy-PUFs, the dynamic exchanges during thermal reprocessing could be promoted by the transesterification of triglyceride linkages of soy segments in the PU networks. Although the bond energy of the carbamide bonds is typically stronger than that of the carbamate bonds, the hard domain could also participate in the dynamic exchanges, partly through the physical rearrangement of hydrogen bonds in carbamide bonds at elevated temperatures.[52,98] Meanwhile, the hard domain could also contain free –OH groups and carbamate bonds due to using short-chain DEA (diethanolamine, DEA) as a crosslinker, enabling transcarbamoylation and subsequent urethane exchanges together with the soft domain. As a result, dynamic exchanges within the PU networks led to another microphase separation behavior during the reprocessing process. In comparison, a more noticeable T_g3 was noted in the converted S-50%Bo (Fig. 6f), suggesting the occurrence of more intensive dynamic exchanges during the converting soy-PUFs to PUSs due to the transesterification contributed from the soy segments. As a result, for S-50%Bo, the T_g1 of PUS (related to the long-chain polyether polyol) became more distinguishable than that of the original F-50%Bo, because some soy segments from the soft domain (T_g1) of the PU networks have undergone topological rearrangements to form T_g3 in the PUS samples.

Typically, topological rearrangement temperature (Tv) was higher than T_g;[54] in the case of flexible PUFs, the onset of glassy-rubbery transition of hard domains triggered Tv.[66] Thermomechanical analysis (TMA) of the sheet samples also revealed their Tvs were about 170 °C (Fig. S5†). However, as we mentioned above, reprocessing of PUF at temperatures above 160 °C could lead to severe degradation of PUSs. On the other hand, all PUF samples displayed significant stress relaxation at lower temperatures around 130 or 150 °C (Fig. S3†), which was greatly higher than T_g1 and close to Tv, indicating sufficient chain mobility even when the hard domains remained partially frozen. Thereby, we selected to reprocess PUFs at 160 °C.

© 2025 The Author(s). Co-published by the Institute of Process Engineering, Chinese Academy of Sciences and the Royal Society of Chemistry

Open Access Article. Published on 22 1403. Downloaded on 10/03/1405 06:34:15 ..
This article is licensed under a Creative Commons Attribution-NonCommercial 3.0 Unported Licence.

As demonstrated above, PUSs were prepared by the foam-to-sheet reprocessing on shredded PUF fragments. Aiming to assess the impact of the initial physical state of PUFs on the quality of the resulting PUSs, we further performed the pulverization process on PUFs using a grinder mill (sieved them to collect particles lower than 1000 μm). These pulverized powders were subjected to the same foam-to-sheet conversion as the shredded fragments, as shown in Fig. S6.† It was found that PUSs made from this pulverizing route (named S-*X*(P)) exhibited similar densities as those sheets made from the shredding route (Table 2). Meanwhile, their mechanical properties (Table S5†) were not significantly different from those of shredded fragments (Table 2). For instance, for S-25%Bo(P) *versus* shredded foams S-25%Bo, the tensile modulus and strength were 46.9 *vs.* 50.9 MPa, 12.2 *vs.* 13.3 MPa, and elongation at breaks were 66% *vs.* 71%, respectively. This suggests that the foam-to-sheet reprocessing of vitrimerized PUFs may not require a complex pulverization to grind them into fine powder form, since the simple shredding process can save energy usage and cost in recycling. On the other hand, in those sheets made from pulverized powders, the mechanical properties and cross-linking degrees (reflected by gel contents in Table S4†) of S-25%50(P) and S-50%50(P) are still inferior to the other 5 PUS samples, demonstrating a similar issue of irreversible cleavage of soy segments during thermal reprocessing in PUS made from shredding route.

3 Conclusion

In summary, vitrimerized soy-PUFs (density = ~40 kg m^{-3}) were produced using commercial soy polyols (Cargill's BiOH 5000 and/or BiOH 5300) to substitute 25 wt% or 50 wt% petrochemical polyether polyol. The effect of soy polyols on the intrinsic mechanical and thermal properties of PUFs was characterized. It was found that the introduction of soy polyols, especially BiOH 5300 with higher OH functionality (3.0), significantly increased the mechanical stiffness of PUFs. For instance, the tensile modulus of F-50%53 (794 kPa) is about 4.3 times that of the F-Control (186 kPa). The use of BiOH 5000 with lower OH functionality (1.7) preserved the mechanical flexibility of PUFs. However, BiOH 5000 adversely reduced the cross-linked network revealed by lower gel contents of PUFs. All the prepared PUFs underwent successful reprocessing into densified PUSs (density = ~1.05 g cm^{-3}) through compression molding at relatively mild conditions (160 °C, 30 min), where the resulting PUSs exhibited decent structural integrity and mechanical properties. For instance, the tensile modulus, tensile strength, and Shore-D hardness of S-50%Bo are 88.7 MPa, 14.9 MPa, and 41, respectively. This could be attributed to the dynamical exchanges inside the PU networks evidenced by the stress relaxation test and DMA. Maintaining a low concentration of DBTDL (~0.5 wt%) and slightly excess –OH groups in the network structure (by keeping –OH to –NCO molar ratio at 1 : 0.98) enabled effective reprocessability. Even the F-Control, *i.e.*, the petrochemical polyether-based PUF prepared in this way, displayed decent reprocessability as S-Control showed proper mechanical properties and gel contents. However, caution should be taken for soy-PUFs to prevent irreversible cleavage of triglyceride linkages beyond dynamic exchanges, especially for those containing BiOH 5000. Challenges remain in the sustainable design of flexible PUFs, notably the need for soy polyols with appropriate OH functionality (around 2–2.5) and homogeneous molecular structures (*e.g.*, low PDI), which are essential for retaining the mechanical flexibility of the cross-linked networks. This consideration was also critical for PU sheet or film products after reprocessing to attain desirable structural integrity and mechanical performance. In general, our case on soy-PUFs offers insight into the development of biobased and recyclable PUFs in terms of facile industrial implementation, especially in the automobile sectors.

4 Experimental

4.1 Materials

Petrochemical long-chain polyether polyol (Dow's Voranol® 4701) with OH value of 34.4 mg KOH g^{-1} and OH functionality of 3.0 is provided by Dow Inc. Two different types of soy polyols (Cargill's BiOH® 5000 and BiOH® 5300) are kindly provided by Cargill Inc, and their OH values and functionalities are 56 mg KOH g^{-1} and 1.7 (for BiOH 5000); 117 mg KOH g^{-1} and 3.0 (for BiOH 5300), respectively. Their synthetic route and chemical structures (Fig. S1†) are deduced according to their technique article.[30] Polymeric methylene diphenyl isocyanate (MDI) isomer mixture (Huntsman's Rubinate® 1820) with NCO content of 32.0% and OH functionality of 2.47, is kindly provided by TRiiSO LLC. Deionized water from the local facility is used as the chemical blowing agent. Silicone-based surfactant (Evonik's Tegostab® B4690) is obtained from Evonik Industries. Diethanolamine (DEA, assay = 98%) as the cross-linking agent with functionality of 3, dibutyltin dilaurate (DBTDL, assay = 95%) as the catalyst, polysorbate (TWEEN® 80) as cell-opener and surfactant with OH value of ~72.5 mg KOH g^{-1} were purchased from Sigma-Aldrich.

4.2 Preparation of PUF

Table 3 gives the formulations of PUFs, and the details of polyols are illustrated in Fig. S1.† The overall molar ratio of equivalent –OH groups (from polyols, water, TWEEN 80, and DEA (the equivalent of –OH groups of DEA is 3)) *versus* –NCO groups (from MDI) was fixed at 1 : 0.98 for all the 7 formulations. Correspondingly, the use of MDI gradually increased due to the replacement of polyether polyol of lower OH value (34.4 mg KOH g^{-1}) by soy polyols of higher OH values (56 and 117 mg KOH g^{-1}). Likewise, the concentration of the DBTDL catalyst was adjusted based on the molar content of carbamate and carbamide bonds in the PUF formulations. Detailed information of PUF compositions with respect to weight percent and equivalent is given in Tables S1 and S2.†

© 2025 The Author(s). Co-published by the Institute of Process Engineering, Chinese Academy of Sciences and the Royal Society of Chemistry

Open Access Article. Published on 22 1403. Downloaded on 10/03/1405 06:34:15 ..
This article is licensed under a Creative Commons Attribution-NonCommercial 3.0 Unported Licence.

Table 3 Formulations of PUFs

Sample code			F-Control[a]	F-25%50[a]	F-25%53[a]	F-25%Bo[a]	F-50%50[a]	F-50%53[a]	F-50%Bo[a]
Component information			Composition (corresponding to 100 phr polyols)						
	Name	Function							
Component-B	Voranol 4701	Petrochemical polyol	100	75	75	75	50	50	50
	BiOH 5000	Soy polyol-1	0	25	0	12.5	50	0	25
	BiOH 5300	Soy polyol-2	0	0	25	12.5	0	50	25
	TWEEN 80	Cell opener & surfactant	1						
	Tegostab B4690	Surfactant	0.5						
	DEA	Crosslinker	1.5						
	DBTDL	Catalyst	0.8	0.82	0.86	0.84	0.83	0.92	0.87
	Water	Blowing agent	3.5						
Component-A	Rubinate 1820	Polyisocyanates (MDI)	63.5	64.7	68.3	66.5	66	73	69.5
Content of soy polyol (wt%)			0	14.5	14.2	14.4	28.8	27.7	28.3

[a] Codes of PUF samples are named according to the selection of soybean polyols (50 stood for BiOH 5000; 53 stood for BiOH 5300; "Bo" stood for both 5000 and 5300) and the content (25% or 50% corresponded to 100 phr polyol).

Prior to curing, all ingredients except the MDI were pre-mixed using a mechanical mixer at 2500 rpm for 6 min to give a viscous blend referred to as component-B. Next, a predetermined amount of MDI (component-A) was poured into component-B and vigorously mixed using a drill mixer at 3000 rpm for 15 s. When the A–B mixture (about 75 grams) started rising, it was immediately transferred into a closed mold (180 × 135 × 60 mm^3, overall ~1500 mL) pre-coated with a wax-dispersion releasing agent and then subjected to a ventilation oven at 80 °C. After shaping and pre-curing in the mold for 8 min, the demolded PUFs were post-cured in the oven at 80 °C for 4 hours. All PUF specimens were conditioned at room temperature for at least 5 days prior to characterization.

4.3 Reprocessing of PUFs into non-porous PUSs

The thermal reprocessability and malleability of PUF, either in the form of shredded pieces or pulverized particles, were demonstrated by converting the foam materials into densified sheet materials *via* compression molding, *i.e.*, the foam-to-sheet conversion. First, PUFs (25 grams) were properly loaded into a 100 × 100 mm^2 male–female mold that was pre-coated with Teflon-aerosol releasing agent and then subjected to hot-press (160 °C), and the compression pressure was gradually increased to 15 MPa over a period of 10 min. After being hot-pressed for 20 min under constant pressure (15 MPa), the mold with specimen was transferred to a cold-press and then pressed at room temperature for 10 min at 1 MPa. The thickness of PUSs obtained was about 2.5 mm. All PUS specimens were conditioned at room temperature for at least 5 days prior to testing.

4.4 Characterizations

Characterization of PUFs. PUFs were first cut *via* a thermal wire cutter from the entire foam blocks and then die stamped with a press to the proper size and shape as needed for testing. The apparent density of PUFs was obtained according to ASTM D3574-A standard, where the dimensions (nominally 50 mm × 50 mm × 25 mm) and mass of samples (5 replicates) were measured to calculate density. The compression force deflection test of PUFs was based on ASTM D3574-C standard (50 mm × 50 mm × 25 mm) and conducted on a universal testing machine (Instron 5565) equipped with a 5 kN load cell. The crosshead speed was 50 mm min^{-1}, and the gauge distance was 25 mm. The tensile test of PUFs followed ASTM D3574-E standard *via* a universal testing machine (Instron 3366) equipped with a 500 N load cell. The crosshead speed was 500 mm min^{-1}, and the gauge length was 59 mm. Specimens were prepared from wire cut sheets that were die stamped with a standard dumbbell shape (ASTM D412 Die A), and the dimensions were 140 × 12 × 10 mm^3. The tear resistance of PUFs was measured using the same universal testing machine mentioned above. The crosshead speed was 500 mm min^{-1}, and the gauge length was 59 mm. Specimens were wire cut and die stamped with a dumbbell shape (ASTM D624 Die C), and the dimensions were 102 × 12.7 × 10 mm^3. The average results of all the mechanical testing were based on 5 replicates.

The wet compression set of PUFs was characterized according to ASTM D3574-L. Samples (50 mm × 50 mm × 25 mm) were held at a 50% compressive strain and then placed in the humidity chamber at 95% relative humidity for 22 h. After the samples were removed from the chamber, they were allowed to decompress for 30 min, and then the thickness was measured. The stress relaxation test on PUFs was performed on a dynamical mechanical analyzer (DMA, TA Q800) equipped with a tension fixture. Samples (about 25 mm × 5 mm × 5 mm) were heated to the test temperature (130, 150, and 170 °C) and equilibrated for 10 minutes. A preload force of 0.001 N was applied to ensure good sample contact. The grip distance was adjusted to 10 mm. During the test, a strain of 5% was applied and maintained, while the relaxation modulus was recorded as a function of time. At the end of the test, a polynomial fit was performed on the resulting curves. The apparent activation energy (E_a) is calculated based on the Arrhenius eqn (1)

© 2025 The Author(s). Co-published by the Institute of Process Engineering, Chinese Academy of Sciences and the Royal Society of Chemistry

Open Access Article. Published on 22 1403. Downloaded on 10/03/1405 06:34:15 ..
This article is licensed under a Creative Commons Attribution-NonCommercial 3.0 Unported Licence.

$$\ln\tau^* = \frac{E_a}{RT} - \ln A \quad (1)$$

where τ^* is relaxation time when the relaxation modulus reaches $1/e$, T is the absolute temperature, A is a pre-exponential factor, and R is the gas constant.

Characterization of PUSs. Sheet specimens (*i.e.*, PUS) were cut by a shear saw and die stamped with the same compression machine into the appropriate size and shape. The density of PUSs was measured according to ASTM D792 standard. Samples with dimensions of 10 mm × 10 mm × 2.5 mm were suspended on the analytical balance and then immersed in water to determine their specific gravity. The Shore D hardness of PUSs was obtained *via* a durometer (Haibao LD-J) following ASTM D2240 standard (about 10 mm × 10 mm × 2.5 mm) with modification. The tensile test of PUSs was based on ASTM D638 standard and conducted on a universal testing machine (Instron 5565) equipped with a 5 kN load cell. The crosshead speed was 50 mm min^{-1}, and the gauge length was 7.62 mm. The specimens (63.5 mm × 3.18 mm × 2.5 mm) were die stamped with a standard dumbbell shape cutter (ASTM D638 type V). The average results of all the mechanical testing were based on 5 replicates.

Other characterizations. The dynamic mechanical properties of both PUFs (about 50.0 mm × 5.0 mm × 5.0 mm) and PUSs (about 10.0 mm × 1.0 mm × 1.0 mm) cut by shear saw were performed on a dynamic mechanical analyzer (DMA, Rheometric Scientific 3E) equipped with a tension fixture. Samples were scanned from −100 °C to 200 °C at a ramp rate of 3 °C min^{-1}. Frequency was set at 1 Hz, and strain was set at 0.1%. Thermal gravimetric analysis (TGA, Mettler Toledo TGA-1) of the samples (~5 mg) was performed under N_2 gas atmosphere, scanning from 50 to 600 °C at a ramp rate of 10 °C min^{-1}. The morphology study was performed on a scanning electron microscope (SEM, FEI Quanta 200F) and a digital optical microscope (Keyence VHX-7000). In order to observe the internal morphology, samples were cryo-fractured after immersion in liquid nitrogen over 30 min. For SEM, samples were coated with gold for ~15 nm before imaging.

Fourier transform infrared (FTIR) spectra were obtained using an IR spectrometer (Thermo Scientific NICOLET iS50) equipped with attenuated total reflection (ATR) mode. The sample was scanned from 650 to 4000 cm^{-1} for 64 scans with a resolution of 4 cm^{-1}. The molecular weights of polyols were characterized by gel permeation chromatography (GPC, Viscotek M305 TDA) using polystyrene standards. The test was performed at 30 °C, and tetrahydrofuran (THF, Fisher Scientific) was used as an eluent with a flow rate of 1 mL min^{-1}.

Gel content and swelling ratio of PUFs and PUSs were determined as follows: a sample of ~250 mg for PUFs and ~500 mg for PUSs (W_0) was immersed into two testing systems for 3 days: (a) methyl ethyl ketone (MEK, Fisher Scientific) at room temperature or (b) boiling toluene (Fisher Scientific) *via* Soxhlet extraction (~120 °C). The swollen samples were weighed (W_g) and later dried in a vacuum oven at 80 °C for 12 h until a constant weight (W_d) was obtained. The gel fraction and swelling ratio were calculated according to the following eqn (2) and (3),

$$\text{Gel fraction (\%)} = W_d/W_0 \quad (2)$$

$$\text{Swelling Ratio} = (W_g - W_d)/W_d \times K + 1 \quad (3)$$

where K is the ratio of the density of the sample *versus* the corresponding solvent (MEK or toluene). At least 3 repeats were performed for each formulation.

Data availability

Data are contained within the article and the ESI,† including (1) analysis of polyols characterized by FTIR and GPC, and comparison between MDI and the F-Control, (2) detailed composition of the 7 PUFs, (3) optical images of PUFs, (4) detailed compression properties of PUFs, (5) detailed gel content and swelling ratios of PUFs and PUSs after reprocessing, (6) stress relaxation of PUFs in different temperature, (7) images of soy-PUFs after reprocessing at excessive temperature and time that illustrate degradation issue, (8) images of PUSs reprocessed from PUFs of pulverized powders; (9) densities and mechanical properties of PUSs reprocessed from PUFs of pulverized powders.

Conflicts of interest

The authors declare no conflict of interest.

Acknowledgements

The authors are grateful for the financial support from the United Soybean Board, Project No. 2333-102-0201 and 2422-106-010. We want to acknowledge Cargill for providing soybean polyols. We also thank Doug Quinn of TRiiSO for providing the MDIs and other chemicals. We want to express thanks to Ford Motor Company's Research and Advanced Engineering's researchers (Sandeep Tamrakar and Robert Bedard) for supporting our experiments.

References

1 N. V. Gama, A. Ferreira and A. Barros-Timmons, Polyurethane foams: Past, present, and future, *Materials*, 2018, **11**, 1841.
2 K. M. Zia, H. N. Bhatti and I. A. Bhatti, Methods for polyurethane and polyurethane composites, recycling and recovery: A review, *React. Funct. Polym.*, 2007, **67**, 675–692.
3 B. Eling, Ž. Tomović and V. Schädler, Current and future trends in polyurethanes: An industrial perspective, *Macromol. Chem. Phys.*, 2020, **221**, 2000114.
4 M. DeBolt, A. Kiziltas, D. Mielewski, S. Waddington and M. J. Nagridge, Flexible polyurethane foams formulated with polyols derived from waste carbon dioxide, *J. Appl. Polym. Sci.*, 2016, **133**, 44086.

© 2025 The Author(s). Co-published by the Institute of Process Engineering, Chinese Academy of Sciences and the Royal Society of Chemistry

Open Access Article. Published on 22 1403. Downloaded on 10/03/1405 06:34:15 ..
This article is licensed under a Creative Commons Attribution-NonCommercial 3.0 Unported Licence.

5 F. M. de Souza, J. Choi, T. Ingsel and R. K. Gupta, in *Nanotechnology in the Automotive Industry*, Elsevier, 2022, pp. 105–129.
6 D. F. Mielewski, C. M. Flanigan, C. Perry, M. J. Zaluzec and P. C. Killgoar, Soybean oil auto applications: Developing flexible polyurethane foam formulations containing functionalized soybean oil for automotive applications, *Ind. Biotechnol.*, 2005, **1**, 32–34.
7 G. S. Dhaliwal, S. Anandan, K. Chandrashekhara, N. Dudenhoeffer and P. Nam, Fabrication and testing of soy-based polyurethane foam for insulation and structural applications, *J. Polym. Environ.*, 2019, **27**, 1897–1907.
8 S. D. Bote, A. Kiziltas, I. Scheper, D. Mielewski and R. Narayan, Biobased flexible polyurethane foams manufactured from lactide-based polyester-ether polyols for automotive applications, *J. Appl. Polym. Sci.*, 2021, **138**, 50690.
9 C. Liang, U. R. Gracida-Alvarez, E. T. Gallant, P. A. Gillis, Y. A. Marques, G. P. Abramo, T. R. Hawkins and J. B. Dunn, Material flows of polyurethane in the United States, *Environ. Sci. Technol.*, 2021, **55**, 14215–14224.
10 J. Datta and E. Głowińska, Effect of hydroxylated soybean oil and bio-based propanediol on the structure and thermal properties of synthesized bio-polyurethanes, *Ind. Crops Prod.*, 2014, **61**, 84–91.
11 M. Ghasemlou, F. Daver, E. P. Ivanova and B. Adhikari, Polyurethanes from seed oil-based polyols: A review of synthesis, mechanical and thermal properties, *Ind. Crops Prod.*, 2019, **142**, 111841.
12 E. Mendiburu-Valor, T. Calvo-Correas, L. Martin, I. Harismendy, C. Peña-Rodriguez and A. Eceiza, Synthesis and characterization of sustainable polyurethanes from renewable and recycled feedstocks, *J. Cleaner Prod.*, 2023, **400**, 136749.
13 L. L. Monteavaro, E. O. da Silva, A. P. O. Costa, D. Samios, A. E. Gerbase and C. L. Petzhold, Polyurethane networks from formiated soy polyols: Synthesis and mechanical characterization, *J. Am. Oil Chem. Soc.*, 2005, **82**, 365–371.
14 A. Guo, I. Javni and Z. Petrovic, Rigid polyurethane foams based on soybean oil, *J. Appl. Polym. Sci.*, 2000, **77**, 467–473.
15 M. Desroches, M. Escouvois, R. Auvergne, S. Caillol and B. Boutevin, From vegetable oils to polyurethanes: Synthetic routes to polyols and main industrial products, *Polym. Rev.*, 2012, **52**, 38–79.
16 M. A. Sawpan, Polyurethanes from vegetable oils and applications: A review, *J. Polym. Res.*, 2018, **25**, 184.
17 P. Furtwengler and L. Avérous, Renewable polyols for advanced polyurethane foams from diverse biomass resources, *Polym. Chem.*, 2018, **9**, 4258–4287.
18 R. Gu, S. Konar and M. Sain, Preparation and characterization of sustainable polyurethane foams from soybean oils, *J. Am. Oil Chem. Soc.*, 2012, **89**, 2103–2111.
19 P. Rojek and A. Prociak, Effect of different rapeseed-oil-based polyols on mechanical properties of flexible polyurethane foams, *J. Appl. Polym. Sci.*, 2012, **125**, 2936–2945.
20 H. Pawlik and A. Prociak, Influence of palm oil-based polyol on the properties of flexible polyurethane foams, *J. Polym. Environ.*, 2012, **20**, 438–445.
21 J. Peyrton and L. Avérous, Structure-properties relationships of cellular materials from biobased polyurethane foams, *Mater. Sci. Eng., R*, 2021, **145**, 100608.
22 A. Prociak, M. Kurańska, U. Cabulis, J. Ryszkowska, M. Leszczyńska, K. Uram and M. Kirpluks, Effect of bio-polyols with different chemical structures on foaming of polyurethane systems and foam properties, *Ind. Crops Prod.*, 2018, **120**, 262–270.
23 Z. S. Petrović, Polyurethanes from vegetable oils, *Polym. Rev.*, 2008, **48**, 109–155.
24 C. Zhang, T. F. Garrison, S. A. Madbouly and M. R. Kessler, Recent advances in vegetable oil-based polymers and their composites, *Prog. Polym. Sci.*, 2017, **71**, 91–143.
25 D. Ji, Z. Fang, W. He, Z. Luo, X. Jiang, T. Wang and K. Guo, Polyurethane rigid foams formed from different soy-based polyols by the ring opening of epoxidised soybean oil with methanol, phenol, and cyclohexanol, *Ind. Crops Prod.*, 2015, **74**, 76–82.
26 Z. S. Petrovic, I. X. Javni, A. Zlatanic and A. X. Guo, *US Pat.*, US8153746B2, 2012.
27 Z. Petrovic, I. Javni, A. Guo and W. Zhang, *US Pat.*, US6433121B1, 2002.
28 Z. Petrovic, A. Guo and I. Javni, *US Pat.*, US6107433, 2000.
29 F. Yang, H. Yu, Y. Deng and X. Xu, Synthesis and characterization of different soybean oil-based polyols with fatty alcohol and aromatic alcohol, *e-Polym.*, 2021, **21**, 491–499.
30 T. W. Abraham, in *Biobased Monomers, Polymers, and Materials*, ACS Publications, 2012, pp. 165–181.
31 C. Zhang and M. R. Kessler, Bio-based polyurethane foam made from compatible blends of vegetable-oil-based polyol and petroleum-based polyol, *ACS Sustainable Chem. Eng.*, 2015, **3**, 743–749.
32 A. Campanella, L. Bonnaillie and R. Wool, Polyurethane foams from soyoil-based polyols, *J. Appl. Polym. Sci.*, 2009, **112**, 2567–2578.
33 L. Zhang, H. K. Jeon, J. Malsam, R. Herrington and C. W. Macosko, Substituting soybean oil-based polyol into polyurethane flexible foams, *Polymer*, 2007, **48**, 6656–6667.
34 H. Nurul 'Ain, T. T. N. Maznee, M. Norhayati, M. M. Noor, S. Adnan, P. K. Devi, S. M. Norhisham, S. Yeong, A. Hazimah and I. Campara, Natural palm olein polyol as a replacement for polyether polyols in viscoelastic polyurethane foam, *J. Am. Oil Chem. Soc.*, 2016, **93**, 983–993.
35 S. Das, M. Dave and G. Wilkes, Characterization of flexible polyurethane foams based on soybean-based polyols, *J. Appl. Polym. Sci.*, 2009, **112**, 299–308.
36 G. S. Dhaliwal, S. Anandan, K. Chandrashekhara, J. Lees and P. Nam, Development and characterization of polyurethane foams with substitution of polyether polyol with soy-based polyol, *Eur. Polym. J.*, 2018, **107**, 105–117.
37 F. Quadrini, D. Bellisario and L. Santo, Recycling of thermoset polyurethane foams, *Polym. Eng. Sci.*, 2013, **53**, 1357–1363.

© 2025 The Author(s). Co-published by the Institute of Process Engineering, Chinese Academy of Sciences and the Royal Society of Chemistry

Open Access Article. Published on 22 1403. Downloaded on 10/03/1405 06:34:15 ..
This article is licensed under a Creative Commons Attribution-NonCommercial 3.0 Unported Licence.

38 W. Yang, Q. Dong, S. Liu, H. Xie, L. Liu and J. Li, Recycling and disposal methods for polyurethane foam wastes, *Procedia Environ. Sci.*, 2012, **16**, 167–175.
39 D. Simón, A. Borreguero, A. De Lucas and J. Rodríguez, Recycling of polyurethanes from laboratory to industry, a journey towards the sustainability, *Waste Manage.*, 2018, **76**, 147–171.
40 A. Hulme and T. Goodhead, Cost effective reprocessing of polyurethane by hot compression moulding, *J. Mater. Process. Technol*, 2003, **139**, 322–326.
41 Y. Deng, R. Dewil, L. Appels, R. Ansart, J. Baeyens and Q. Kang, Reviewing the thermo-chemical recycling of waste polyurethane foam, *J. Environ. Manage.*, 2021, **278**, 111527.
42 S. A. Madbouly, Novel recycling processes for thermoset polyurethane foams, *Curr. Opin. Green Sustainable Chem.*, 2023, **42**, 100835.
43 F. Recupido, G. C. Lama, S. Steffen, C. Dreyer, H. Seidlitz, V. Russo, M. Lavorgna, F. D. L. Bossa, S. Silvano and L. Boggioni, Efficient recycling pathway of bio-based composite polyurethane foams via sustainable diamine, *Ecotoxicol. Environ. Saf.*, 2024, **269**, 115758.
44 J. Borda, G. Pásztor and M. Zsuga, Glycolysis of polyurethane foams and elastomers, *Polym. Degrad. Stab.*, 2000, **68**, 419–422.
45 M. Grdadolnik, A. Drinčić, A. Oreški, O. C. Onder, P. Utroša, D. Pahovnik and E. Žagar, Insight into chemical recycling of flexible polyurethane foams by acidolysis, *ACS Sustainable Chem. Eng.*, 2022, **10**, 1323–1332.
46 M. Sun, D. T. Sheppard, J. P. Brutman, A. Alsbaiee and W. R. Dichtel, Green catalysts for reprocessing thermoset polyurethanes, *Macromolecules*, 2023, **56**, 6978–6987.
47 J. Liu, J. He, R. Xue, B. Xu, X. Qian, F. Xin, L. M. Blank, J. Zhou, R. Wei and W. Dong, Biodegradation and up-cycling of polyurethanes: Progress, challenges, and prospects, *Biotechnol. Adv.*, 2021, **48**, 107730.
48 J. Liu, J. Liu, B. Xu, A. Xu, S. Cao, R. Wei, J. Zhou, M. Jiang and W. Dong, Biodegradation of polyether-polyurethane foam in yellow mealworms (tenebrio molitor) and effects on the gut microbiome, *Chemosphere*, 2022, **304**, 135263.
49 D. Montarnal, M. Capelot, F. Tournilhac and L. Leibler, Silica-like malleable materials from permanent organic networks, *Science*, 2011, **334**, 965–968.
50 W. Gao, M. Bie, Y. Quan, J. Zhu and W. Zhang, Self-healing, reprocessing and sealing abilities of polysulfide-based polyurethane, *Polymer*, 2018, **151**, 27–33.
51 D. J. Fortman, R. L. Snyder, D. T. Sheppard and W. R. Dichtel, Rapidly reprocessable cross-linked polyhydroxyurethanes based on disulfide exchange, *ACS Macro Lett.*, 2018, **7**, 1226–1231.
52 T. Li, Z. Xie, J. Xu, Y. Weng and B.-H. Guo, Design of a self-healing cross-linked polyurea with dynamic cross-links based on disulfide bonds and hydrogen bonding, *Eur. Polym. J.*, 2018, **107**, 249–257.
53 S. M. Kim, H. Jeon, S. H. Shin, S. A. Park, J. Jegal, S. Y. Hwang, D. X. Oh and J. Park, Superior toughness and fast self-healing at room temperature engineered by transparent elastomers, *Adv. Mater.*, 2018, **30**, 1705145.
54 Y. Tao, X. Liang, J. Zhang, I. M. Lei and J. Liu, Polyurethane vitrimers: Chemistry, properties and applications, *J. Polym. Sci.*, 2023, **61**, 2233–2253.
55 N. Zheng, Y. Xu, Q. Zhao and T. Xie, Dynamic covalent polymer networks: A molecular platform for designing functions beyond chemical recycling and self-healing, *Chem. Rev.*, 2021, **121**, 1716–1745.
56 N. Zheng, Z. Fang, W. Zou, Q. Zhao and T. Xie, Thermoset shape-memory polyurethane with intrinsic plasticity enabled by transcarbamoylation, *Angew. Chem.*, 2016, **128**, 11593–11597.
57 C. Bakkali-Hassani, D. Berne, V. Ladmiral and S. Caillol, Transcarbamoylation in polyurethanes: Underestimated exchange reactions?, *Macromolecules*, 2022, **55**, 7974–7991.
58 W. Denissen, G. Rivero, R. Nicolaÿ, L. Leibler, J. M. Winne and F. E. Du Prez, Vinylogous urethane vitrimers, *Adv. Funct. Mater.*, 2015, **25**, 2451–2457.
59 D. T. Sheppard, K. Jin, L. S. Hamachi, W. Dean, D. J. Fortman, C. J. Ellison and W. R. Dichtel, Reprocessing postconsumer polyurethane foam using carbamate exchange catalysis and twin-screw extrusion, *ACS Cent. Sci.*, 2020, **6**, 921–927.
60 H. Ying, Y. Zhang and J. Cheng, Dynamic urea bond for the design of reversible and self-healing polymers, *Nat. Commun.*, 2014, **5**, 1–9.
61 D. J. Fortman, J. P. Brutman, C. J. Cramer, M. A. Hillmyer and W. R. Dichtel, Mechanically activated, catalyst-free polyhydroxyurethane vitrimers, *J. Am. Chem. Soc.*, 2015, **137**, 14019–14022.
62 Y. Zhang, H. Ying, K. R. Hart, Y. Wu, A. J. Hsu, A. M. Coppola, T. A. Kim, K. Yang, N. R. Sottos and S. R. White, Malleable and recyclable poly (urea-urethane) thermosets bearing hindered urea bonds, *Adv. Mater.*, 2016, **28**, 7646–7651.
63 H. Ying, Y. Zhang and J. Cheng, Dynamic urea bond for the design of reversible and self-healing polymers, *Nat. Commun.*, 2014, **5**, 3218.
64 J. P. Brutman, D. J. Fortman, G. X. De Hoe, W. R. Dichtel and M. A. Hillmyer, Mechanistic study of stress relaxation in urethane-containing polymer networks, *J. Phys. Chem. B*, 2019, **123**, 1432–1441.
65 A. Kiziltas, D. F. Mielewski, W. Liu and J. Zhang, *US Pat.*, US2023/0406988A1, 2023.
66 W. Liu, Y.-C. Chang, C. Hao, H. Liu, J. Zhang, D. Mielewski and A. Kiziltas, Improving thermal reprocessability of commercial flexible polyurethane foam by vitrimer modification of the hard segments, *ACS Appl. Polym. Mater.*, 2022, **4**, 5056–5067.
67 N. V. Gama, B. Soares, C. S. Freire, R. Silva, C. P. Neto, A. Barros-Timmons and A. Ferreira, Bio-based polyurethane foams toward applications beyond thermal insulation, *Mater. Des.*, 2015, **76**, 77–85.
68 S. Bandyopadhyay-Ghosh, S. B. Ghosh and M. Sain, Synthesis of soy-polyol by two step continuous route and development of soy-based polyurethane foam, *J. Polym. Environ.*, 2010, **18**, 437–442.

© 2025 The Author(s). Co-published by the Institute of Process Engineering, Chinese Academy of Sciences and the Royal Society of Chemistry

Open Access Article. Published on 22 1403. Downloaded on 10/03/1405 06:34:15 ..
This article is licensed under a Creative Commons Attribution-NonCommercial 3.0 Unported Licence.

69 X. Luo, A. Mohanty and M. Misra, Lignin as a reactive reinforcing filler for water-blown rigid biofoam composites from soy oil-based polyurethane, *Ind. Crops Prod.*, 2013, **47**, 13–19.
70 L. Jiao, H. Xiao, Q. Wang and J. Sun, Thermal degradation characteristics of rigid polyurethane foam and the volatile products analysis with TG-FTIR-MS, *Polym. Degrad. Stab.*, 2013, **98**, 2687–2696.
71 N. Sarier and E. Onder, Thermal characteristics of polyurethane foams incorporated with phase change materials, *Thermochim. Acta*, 2007, **454**, 90–98.
72 P. K. Pillai, S. Li, L. Bouzidi and S. S. Narine, Metathesized palm oil polyol for the preparation of improved bio-based rigid and flexible polyurethane foams, *Ind. Crops Prod.*, 2016, **83**, 568–576.
73 A. Bryśkiewicz, M. Zieleniewska, K. Przyjemska, P. Chojnacki and J. Ryszkowska, Modification of flexible polyurethane foams by the addition of natural origin fillers, *Polym. Degrad. Stab.*, 2016, **132**, 32–40.
74 E. Yılgör, İ. Yılgör and E. Yurtsever, Hydrogen bonding and polyurethane morphology. I. Quantum mechanical calculations of hydrogen bond energies and vibrational spectroscopy of model compounds, *Polymer*, 2002, **43**, 6551–6559.
75 L.-S. Teo, C.-Y. Chen and J.-F. Kuo, Fourier transform infrared spectroscopy study on effects of temperature on hydrogen bonding in amine-containing polyurethanes and poly (urethane– urea) s, *Macromolecules*, 1997, **30**, 1793–1799.
76 M. J. Elwell, A. J. Ryan, H. J. Grünbauer and H. C. Van Lieshout, An FT ir study of reaction kinetics and structure development in model flexible polyurethane foam systems, *Polymer*, 1996, **37**, 1353–1361.
77 N. Luo, D.-N. Wang and S.-K. Ying, Hydrogen-bonding properties of segmented polyether poly (urethane urea) copolymer, *Macromolecules*, 1997, **30**, 4405–4409.
78 I. Izarra, A. Borreguero, I. Garrido, J. Rodríguez and M. Carmona, Comparison of flexible polyurethane foams properties from different polymer polyether polyols, *Polym. Test.*, 2021, **100**, 107268.
79 A. A. Septevani, D. A. Evans, C. Chaleat, D. J. Martin and P. K. Annamalai, A systematic study substituting polyether polyol with palm kernel oil based polyester polyol in rigid polyurethane foam, *Ind. Crops Prod.*, 2015, **66**, 16–26.
80 S. Tan, T. Abraham, D. Ference and C. W. Macosko, Rigid polyurethane foams from a soybean oil-based Polyol, *Polymer*, 2011, **52**, 2840–2846.
81 G. Harikrishnan, T. U. Patro and D. Khakhar, Polyurethane foam– clay nanocomposites: Nanoclays as cell openers, *Ind. Eng. Chem. Res.*, 2006, **45**, 7126–7134.
82 D. Riyapan, A. Saetung and N. Saetung, A novel rigid pu foam based on modified used palm oil as sound absorbing material, *J. Polym. Environ.*, 2019, **27**, 1693–1708.
83 S. Ju, A. Lee, Y. Shin, H. Jang, J.-W. Yi, Y. Oh, N.-J. Jo and T. Park, Preventing the collapse behavior of polyurethane foams with the addition of cellulose nanofiber, *Polymers*, 2023, **15**, 1499.
84 M. Bedell, M. Brown, A. Kiziltas, D. Mielewski, S. Mukerjee and R. Tabor, A case for closed-loop recycling of post-consumer PET for automotive foams, *Waste Manage.*, 2018, **71**, 97–108.
85 N. E. Marcovich, M. Kurańska, A. Prociak, E. Malewska and S. Bujok, The effect of different palm oil-based bio-polyols on foaming process and selected properties of porous polyurethanes, *Polym. Int.*, 2017, **66**, 1522–1529.
86 S. Adnan, M. T. Tuan Noor, N. H. 'Ain, K. P. Devi, N. S. Mohd, Y. Shoot Kian, Z. B. Idris, I. Campara, C. M. Schiffman and K. Pietrzyk, Impact of the hard-segment concentration on highly resilient polyurethane foams based on palm olein polyol, *J. Appl. Polym. Sci.*, 2017, **134**, 45440.
87 L. Ugarte, A. Saralegi, R. Fernández, L. Martín, M. A. Corcuera and A. Eceiza, Flexible polyurethane foams based on 100% renewably sourced polyols, *Ind. Crops Prod.*, 2014, **62**, 545–551.
88 C. S. Wang, L. T. Yang, B. L. Ni and G. Shi, Polyurethane networks from different soy-based polyols by the ring opening of epoxidized soybean oil with methanol, glycol, and 1, 2-propanediol, *J. Appl. Polym. Sci.*, 2009, **114**, 125–131.
89 J. John, M. Bhattacharya and R. B. Turner, Characterization of polyurethane foams from soybean oil, *J. Appl. Polym. Sci.*, 2002, **86**, 3097–3107.
90 A. Zlatanić, C. Lava, W. Zhang and Z. S. Petrović, Effect of structure on properties of polyols and polyurethanes based on different vegetable oils, *J. Polym. Sci., Part B: Polym. Phys.*, 2004, **42**, 809–819.
91 M. A. Mohd Noor, V. Sendijarevic, S. S. Hoong, I. Sendijarevic, T. N. M. Tuan Ismail, N. A. Hanzah, N. Mohd Noor, K. D. Poo Palam, R. Ghazali and H. Abu Hassan, Molecular weight determination of palm olein polyols by gel permeation chromatography using polyether polyols calibration, *J. Am. Oil Chem. Soc.*, 2016, **93**, 721–730.
92 A. Cifarelli, L. Boggioni, A. Vignali, I. Tritto, F. Bertini and S. Losio, Flexible polyurethane foams from epoxidized vegetable oils and a bio-based diisocyanate, *Polymers*, 2021, **13**, 612.
93 X.-Z. Wang, M.-S. Lu, J.-B. Zeng, Y. Weng and Y.-D. Li, Malleable and thermally recyclable polyurethane foam, *Green Chem.*, 2021, **23**, 307–313.
94 A. Bandegi, M. Montemayor and I. Manas-Zloczower, Vitrimerization of rigid thermoset polyurethane foams: A mechanochemical method to recycle and reprocess thermosets, *Polym. Adv. Technol.*, 2022, **33**, 3750–3758.
95 J. van Aart, J. den Doelder and J. P. Heuts, Reprocessing polyurethane foam using dynamic covalent chemistry in extrusion, *J. Appl. Polym. Sci.*, 2024, **141**, e54941.
96 J. Li, H. Zhu, D. Fang, X. Huang, C. Zhang and Y. Luo, Mechanochemistry recycling of polyurethane foam using urethane exchange reaction, *J. Environ. Chem. Eng.*, 2023, **11**, 110269.
97 S. Kim, K. Li, A. Alsbaiee, J. P. Brutman and W. R. Dichtel, Circular reprocessing of thermoset polyurethane foams, *Adv. Mater.*, 2023, **35**, 2305387.
98 T. Li, C. Zhang, Z. Xie, J. Xu and B.-H. Guo, A multi-scale investigation on effects of hydrogen bonding on micro-structure and macro-properties in a polyurea, *Polymer*, 2018, **145**, 261–271.

© 2025 The Author(s). Co-published by the Institute of Process Engineering, Chinese Academy of Sciences and the Royal Society of Chemistry